Glucose-Triggered Release Using Enzyme-Gated Mesoporous Silica Nanoparticles

Elena Aznar,[a,b] Reynaldo Villalonga,[c,d] Cristina Giménez,[b,a] Félix Sancenón,[b,e,a] M. Dolores Marcos,[b,e,a] Ramón Martínez-Máñez,[b,e,a] Paula Díez,[c] José M. Pingarrón[c,d] and Pedro Amorós[f]

Chemicals

The chemicals tetraethylorthosilicate (TEOS), *n*-cetyltrimethylammonium bromide (CTABr), sodium hydroxide (NaOH), tris(2,2′-bipyridyl)dichlororuthenium(II) hexahydrate, 3-iodopropyltrimethoxysilane, benzimidazole, triethylamine, glucose, mannose, fructose, galactose, maltose and saccharose were provided by Aldrich. Dry acetonitrile, toluene and ethyl acetate were provided by Scharlau. All reagents were used as received. β-cyclodextrin-modified glucose oxidase (CD-GOx) was synthesized as previously reported.[1]

General Techniques

Powder XRD, TG analysis, elemental analysis, transmission electron microscopy, N_2 adsorption-desorption and UV-visible spectroscopy techniques were used to characterize the prepared materials. X-ray measurements were performed on a Bruker AXS D8 Advance diffractometer using Cu-K_α radiation. Thermo-gravimetric analyses were carried out on a TGA/SDTA 851e Mettler Toledo equipment, using an oxidant atmosphere (Air, 80 mL/min) with a heating program consisting on a heating rate of 10 °C per minute from 393 K to 1273 K and an isothermal heating step at this temperature during 30 minutes. TEM images were taken with a Philips CM10 microscope working at 100 kV. N_2 adsorption-desorption isotherms were recorded on a Micromeritics ASAP2010 automated sorption analyser. The samples were degassed at 120 ºC under vacuum overnight. The specific surface areas were calculated from the adsorption data in the low pressures range using the BET model. Pore size was determined by following the BJH method. UV-visible spectroscopy was carried out with a Lambda 35 UV/vis spectrometer (Perkin-Elmer Instruments).

Synthesis of the silica mesoporous nanoparticles support (SMPS)

The MCM-41 mesoporous nanoparticles were synthesized by the following procedure: *n*-cetyltrimethylammoniumbromide (CTABr, 1.00 g, 2.74 mmol) was first dissolved in 480 mL of deionized water. Then, 3.5 mL of a NaOH 2.00 mol L^{-1} solution was added followed by an adjustment of the temperature to 80 ºC. TEOS (5.00 mL, 22.4 mmol) was then added dropwise to the surfactant solution. The mixture was stirred for 2 hours to give a white precipitate. Finally the solid was collected by centrifugation, washed with deionized water and dried at 70 ºC overnight (MCM-41 as-synthesized). To prepare the final porous material (MCM-41), the as-synthesized solid was calcined at 550 ºC using an oxidant atmosphere for 5 hours in order to remove the template phase.

Synthesis of S1

To synthesize the hybrid solid **S1**, 500 mg of the calcined MCM-41support and 0.30 g (0.04 mmol) of tris(2,2′-bipyridyl)dichlororuthenium(II) hexahydrate were suspended in 25 mL of anhydrous acetonitrile and heated at 120 ºC in a Dean–Stark apparatus to remove the adsorbed water under an inert atmosphere (Ar gas). The suspension was stirred for 24 hours at room temperature with the aim of loading the pores of the MCM-41 scaffolding. After this, an excess of 3-iodopropyltrimethoxysilane (196 µL, 1 mmol) was added and the suspension was stirred for 5.5 hours. The final orange solid (**S1**) was filtered off, washed with 5 mL of acetonitrile and dried at 70 ºC overnight.

Synthesis of S2

To prepare solid **S2**, 500 mg of S1 were suspended in a 40 mL of a saturated solution of benzimidazole in toluene at 80ºC and containing triethylamine (benzimidazol and triethylamine in a 1:3 proportion). The suspension was refluxed and stirred during 72 hours. The final orange solid (**S2**) was filtered off, washed with 40 mL of acetonitrile and dried at 70 ºC overnight.

Synthesis of S3

To prepare solid **S3**, 10 mg of S2 were suspended in a CD-GOx solution (1mL, 1.56 mg/mL). The suspension was stirred during 24 hours at room temperature. The final capped orange solid (**S3**) was centrifuged (7500 rpm, 3 min) and washed with deionized water at pH 7.5 five times.

Release experiments

To perform the release studies, the freshly prepared S3 solid (10 mg) was suspended in 1.5 mL of deionized water at pH 7.5. Then, each batch was prepared taking 150 µL of the suspension and diluting it to 3 mL with deionized water or the corresponding solution at pH 7.5. To monitor the ruthenium complex release, after a fixed time, 0.3 mL of the suspension were filtered off using 0.45 µm PTFE filters and the delivered cargo was registered via the $[Ru(bpy)_3]Cl_2$ absorbance at 453 nm.

Gluconic acid detection

Generated gluconic acid in the filtered aliquots after the triggering event was detected using the colorimetric assay described by Papandreou[2] and used by Ren and Qu.[3] In this experiment, 125 µL of solution 1 (5 $mmolL^{-1}$ EDTA and 0.15 mmolL-1 triethylamine in water) and 12.5 µL of solution 2 (3 $mmolL^{-1}$ NH_2OH in water) were added to 200 µL of the filtered solution. After 25 min of incubation, 62.5 µL of solution 3 (1 $mmolL^{-1}$ HCl, 0.1 $mmolL^{-1}$ $FeCl_3$, and 0.25 $mmolL^{-1}$ CCl_3COOH in water) was added to the above aqueous solution, and the reaction was allowed to proceed for 5 min before spectral measurements. Thus, an increment in the absortion band at 505 nm was observed confirming the gluconic acid presence and the enzyme-mediated conversion of glucose in gluconic acid.

Materials Characterization

Solids **S1** and **S2** were characterized using standard procedures. Figure SI-1 shows powder X-ray diffraction patterns of the as made nanoparticulated MCM-41 support, the free template porous scaffolding and the **S1** and **S2** functionalized materials. Powder XRD of siliceous nanoparticulated MCM-41 as-synthesized (curve a) shows four low-angle reflections typical of a hexagonal array that can be indexed as (100), (110), (200) and (210) Bragg peaks. A significant displacement of the (100) peak in the powder XRD of the nanoparticulated MCM-41 calcined sample is clearly appreciated in curve b, corresponding to an approximate cell contraction of 6 Å. This displacement and the broadening of the (110) and (200) peaks are related to further condensation of silanol groups during the calcination step. Curve c corresponds to the **S1** powder XRD pattern. In this case, a slight intensity decrease and a broadening of the (110) and (200) reflections is observed, most likely related to a loss of contrast due to the filling of the pore voids with the fluorescein dye. Nevertheless, the value and intensity of the (100) peak in this pattern strongly evidences that the loading process with the dye and the further functionalization with 3-iodopropyltrimethoxysilane have not damaged the mesoporous scaffolding. Finally, curve d corresponds to the **S2** powder XRD pattern in which the peak (100) is also observed confirming the preservation of the inorganic structure during all the synthesis process.

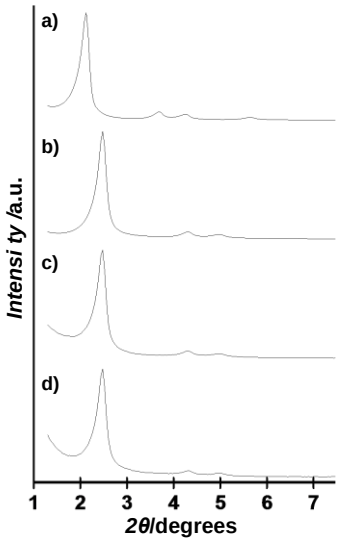

Figure SI-1. Powder X-ray diffraction patterns of the solids (a) MCM-41 as-synthesized (b) calcined MCM-41 (c) solid **S2** containing $[Ru(bpy)_3]Cl_2$ and 3-iodopropyltrimethoxysilane and (d) solid **S2** containing $[Ru(bpy)_3]Cl_2$ and 1-propyl-1-H-benzimidazole.

These results are consistent with TEM studies (Figure SI-2). Thus, Figures SI-2 (a) and (b) show a representative image of the calcined MCM-41 support and **S2** hybrid material, respectively. In these images, the typical hexagonal porosity of MCM-41 matrix can be observed. In addition, the images also evidence the spherical morphology of the particles and their diameter around 100 nm. Figure SI-6 (c) shows a representative image of solid **S3** where the enzyme coating that surrounds the mesoporous nanoparticle can be appreciated and the fact that inorganic structure has been maintained in the course of the materials synthesis is confirmed.

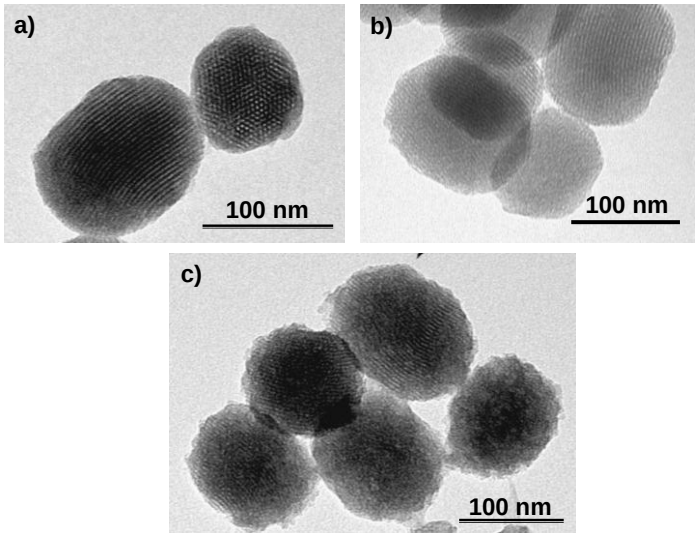

Figure SI-2.TEM images of (a) calcined MCM-41 sample (b) solid **S2** and (c) solid **3** showing the typical hexagonal porosity of the MCM-41 mesoporous matrix.

The N_2 adsorption-desorption isotherms of the nanoparticulated MCM-41 calcined material shows two sharp adsorption steps. The isotherm shows a first step at intermediate P/P_0 value (0.1-0.4) typical of

these solids (see Figure SI-3 curve a). This step can be related to the nitrogen condensation inside the mesopores by capillarity. The absence of a hysteresis loop in this interval and the narrow BJH pore distribution suggest the existence of uniform cylindrical mesopores with a pore volume of 0.76 cm^3 g^{-1} calculated by using the BJH model on the adsorption branch of the isotherm. The application of the BET model resulted in a value for the total specific surface of 1042 m^2/g. From the powder XRD, porosimetry and TEM studies, the a_0 cell parameter (3.56 nm), the pore diameter (2.38 nm) and a value for the wall thickness (1.18 nm) were calculated. In addition to this adsorption step associated to the micelle generated mesopores, a second feature appears in the isotherm at a high relative pressure ($P/P_0 > 0.75$). This second step corresponds to the filling of the large voids among the particles that must be considered as a textural-like porosity. In this case, curves show a characteristic H1 hysteresis loop and a wide pore size distribution.

The N_2 adsorption-desorption isotherm of **S2** is typical of mesoporous systems with filled mesopores (see Figure SI-3 curve b) and a significant decrease in the N_2 volume adsorbed and surface area (60.4 m^2/g) is observed. The most relevant feature is the absence of a sharp step at low-medium relative pressure ($0.1 < P/P_0 < 0.4$). In fact, this solid shows flat curves in that region when compared (at the same scale) to those of the MCM-41 parent material, which indicates a significant pore blocking and the subsequent absence of appreciable mesoporosity. Additionally, the curve shows a N_2 adsorption at high relative pressure similar to the calcined MCM-41, confirmig that the textural porosity is preserved.

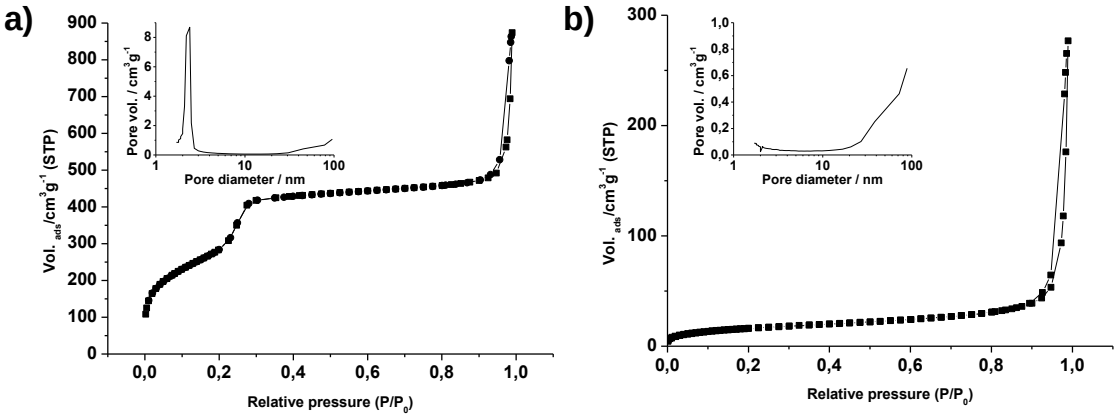

Figure SI-3. Nitrogen adsorption-desorption isotherms for (a) MCM-41 mesoporous material (b) **S2** material. Insets: Pore size distribution of the corresponding material.

BET specific surface values, pore volumes and pore sizes calculated from the N_2 adsorption-desorption isotherms for MCM-41and **S2** are listed in Table 1.

Table 1. BET specific surface values, pore volumes and pore sizes calculated from the N_2 adsorption-desorption isotherms for selected materials.

	S_{BET} (m^2g^{-1})	BJH pore ($P/P_0 < 0.4$)[a] (nm)	BJH pore ($P/P_0 > 0.4$)[b] (nm)	Total pore volume[c] (cm^3g^{-1})	Pore volume ($P/P_0 < 0.4$)[d] (cm^3 g^{-1})	Pore volume ($P/P_0 > 0.4$)[e] (cm^3 g^{-1})
MCM-41	1042.1	2.38	50.78	1.16	0.76	0.40
S2	60.4	--	49.79	0.30	0.05	0.25

[a] Pore size estimated by using the BJH model applied on the adsorption branch of the isotherm, for $P/P_0 < 0.4$, which can be associated to the surfactant generated mesopores.
[b] Medium pore size estimated by using the BJH model applied on the adsorption branch of the isotherm, for $P/P_0 > 0.4$, which can be associated to the textural porosity.
[c] Total pore volume according to the BJH model.
[d] Pore volume for $P/P_0 < 0.4$, which can be associated to the surfactant generated mesopores.
[e] Pore volume for $P/P_0 > 0.4$, which can be associated to the textural porosity.

Ruthenium complex, 3-iodopropyl and 1-propyl-1-H-benzimidazole content in the prepared solids **S1,** and **S2** were determined by elemental analysis and thermogravimetric studies. Content values are detailed in Table 2.

Table 2. Ruthenium complex, 3-iodopropyl and 1-propyl-1-H-benzimidazole content in the prepared solids **S1** and **S2** in % wt.

Solid	**%$_{[Ru(bpy)3]2+}$**	**%$_{3\text{-iodopropyl}}$**	**%$_{1\text{-propyl-1-H-benzimidazole}}$**
S1	19.7	2.2	-
S2	16.1	-	5.2

Taking into account that normal density of silanol groups in silica materials is 6 Si-OH nm^{-2} and that the reactive molecule had three reactive methoxy groups, the maximum density of octadecyl chains in the hybrid solids would be around 2 or 3 molecules per nm^2. From the content of octadecyl, it can be calculated that it is necessary around 104-156 nm^2 of surface to anchor all the 3-iodopropyl chains. As typical external surface for a nanoparticulated MCM-41 solid is ca.70 m^2g^{-1}, it is calculated that between 34-86 nm^2 of internal surface would be modified with 3-iodopropyl chain. From TEM, we estimated that nanoparticles diameter was ca. 100 nm. Thus, the average mesopore length would also be 100 nm. Taking into account that each mesopores has two entrances, we can estimate that 3-iodoprpyl chain have penetrated and functionalized around 3.1 nm deep, allowing 93.8 nm without internal functionalization. From calculated data, it can be concluded that although 3-iodopropil chain could have slightly penetrated inside of the pores, its localization was reduced and limited by the presence of $[Ru(bpy)_3]Cl_2$ molecules in the pore voids.

[1] M. Holzinger, L. Bouffier, R. Villalonga, S. Cosnier, Biosensors and Bioelectronics 2009, 24, 1128–1134
[2] E.T. Rakitzis, P. Papandreou, Chem-Biol Interact 1998, 113, 205-216
[3] Y. Lin, Z. Li, Z. Chen, J. Ren, X. Qu, Biomaterials 2013, 34, 2600-2010